ELSEVIER

The low frequency vibrational modes of green fluorescent proteins

V. Tozzini [a,*], A.R. Bizzarri [b], V. Pellegrini [a], R. Nifosì [a], P. Giannozzi [a], A. Iuliano [c], S. Cannistraro [b], F. Beltram [a]

[a] *NEST-INFM and Scuola Normale Superiore, Piazza dei Cavalieri 7, I-56126 Pisa, Italy*
[b] *INFM, Dip. di Scienze Ambientali, Università della Tuscia, Largo dell'Università, I-01100 Viterbo, Italy*
[c] *Università di Pisa, dip. di Chimica e Chimica Industriale, via Risorgimento 35, I-56100 Pisa, Italy*

Abstract

We report the observation and analysis of the low frequency vibrational modes of green fluorescent proteins (GFPs). Our study exploits the surface enhanced Raman scattering technique, which allowed the analysis of the vibrational modes of the proteins down to 300 cm^{-1}. Here we present results on two GFP mutants, namely S65T/F64L GFP (EGFP) and S65T/F64L/T203Y GFP (E^{2}GFP). These particularly bright mutants display almost inverted population ratio of anionic (B) to neutral (A) forms of the chromophore. By comparing the vibrational spectrum of the proteins with that of a synthetic model chromophore in solution and with the aid of first principle calculations based on density functional theory, we identify the Raman active bands in this region of frequencies. A dominant collective mode at 720 cm^{-1} is found and assigned to a collective planar deformation of the chromophore. Low frequency vibrational modes belonging specifically to A and/or B structural configurations are also identified. This work demonstrates the possibility of monitoring the structural sub-states of GFPs through vibrational spectroscopy in a range of frequencies where collective modes peculiar of the double ring structure of the chromophore lie.
© 2002 Elsevier Science B.V. All rights reserved.

Keywords: Green fluorescent proteins; Surface enhanced Raman scattering; Density functional theory

1. Introduction

In the last decade, green fluorescent proteins (GFPs) have become increasingly important tools in molecular biology, medicine and cell biology [1,2]. A bright intrinsic fluorescence and the possibility of genetically fusing these proteins to others without affecting their functionality, made wild type (WT) GFP and its photo-active mutants widespread fluorescent markers in living cells [2–4]. The 4-(*p*-hydroxybenzylidene)-imidazolidin-5-one chromophore autocatalitically forming during the protein folding by the cyclization of three consecutive amino-acids (S65-Y66-G67 in WT) is protected from the outside by a relatively

---

* Corresponding author. Tel.: +39-050-509-412; fax: +39-050-509-417.

E-mail address: tozzini@nest.sns.it (V. Tozzini).

rigid and stable β-barrel envelope [5,6]. GFPs exist in two thermodynamically stable states absorbing light at different wavelengths, usually called state A (398 nm in WT) and state B (480 nm in WT) and containing phenolic and phenolate chromophore, respectively [7]. Other non-fluorescent structural states must be invoked to explain GFP photo-dynamics and in particular the on-off blinking and photo-bleaching behavior [8]. Details of the structural changes connecting states A and B with dark configurations, however, are still unclear, although the *cis–trans* isomerization of the chromophore has been proposed to be involved in non-radiative relaxation and photo-bleaching dynamics [9–11]. In addition, amino-acid mutations in the active site can modify the structure of the hydrogen bond network connecting the chromophore with the protein environment. These substitutions lead to changes in absorption/emission wavelengths, in the relative population of A and B states and in the photo-dynamics.

Vibrational spectroscopy can be successfully used to study structural properties and dynamical changes in proteins. For instance, Fourier Transform InfraRed (IR) spectroscopy [12] revealed changes in the WT-GFP vibrational spectrum in the 1000–1700 cm^{-1} range upon A–B photo-conversion. A few Raman studies on highly concentrated GFP samples were also performed. In order to increase the ratio between the Raman signal and the fluorescence background different strategies were exploited. In particular, near-IR excitation was used for a selective intensity enhancement of the vibrational bands originating in the chromophore over other protein modes [13]. Alternatively, GFP samples were resonantly excited in the blue wing of the absorption spectrum, to obtain large Raman intensities comparable to the fluorescence background [14]. These studies were mainly focused on the high-wavenumber region ($\geqslant 1000$ cm^{-1}), where the most intense Raman signals appear. The low frequency region is still almost unexplored. Investigations in this region, however, are of particular interest and can reveal peculiar collective vibrations associated to structural changes in the active-site configuration. This was recently shown by some of us in ultra-fast pump-and-probe op-

tical spectroscopy experiments where vibrational bands around 500 cm^{-1} corresponding to a collective GFP chromophore mode correlated to the electronic photo-excitation [15] were observed. A key requirement towards the exploitation of such low frequency vibrations for monitoring structural changes in GFPs is the experimental observation and theoretical identification of the corresponding vibrational modes. Their analysis in conventional Raman spectroscopy, however, is hindered by the high background signal associated to intrinsic luminescence and to the stray light which obscures the manifestation of the modes in this low frequency region.

Here we successfully exploit surface enhanced Raman scattering (SERS) to unravel the GFP vibrational pattern in the range 300–1200 cm^{-1}. We report a comparison between protein SERS spectra and those relative to a synthetic model chromophore in solution. These data are complemented by an analysis based on first principle calculations, which allows us to identify the SERS active modes and associate them to specific patterns of vibrations. We present the results of two mutants, namely EGFP (F64L/S65T) [16] and E^2GFP (F64L/S65T/T203Y) [17], which are mainly stabilized in states B and A, respectively. This allows the identification of some vibrational fingerprint modes which are peculiar to the different structural configuration of anionic and neutral states. The results here reported open new possibilities of monitoring the conformational changes of the chromophore environment during the photo-dynamics.

2. Materials and methods

2.1. Synthesis of the model chromophore

The model chromophore (1) was prepared in two steps as shown in Fig. 1. According to the Erlenmeyer azlactone synthesis [18] 4-acethoxy-benzaldehyde (2) was reacted with a slight excess of *N*-acetylglycine (3) in the presence of acetic anhydride and anhydrous sodium acetate at the reflux for three hours, to afford the azlactone (4). This product was obtained in 70% yield and was
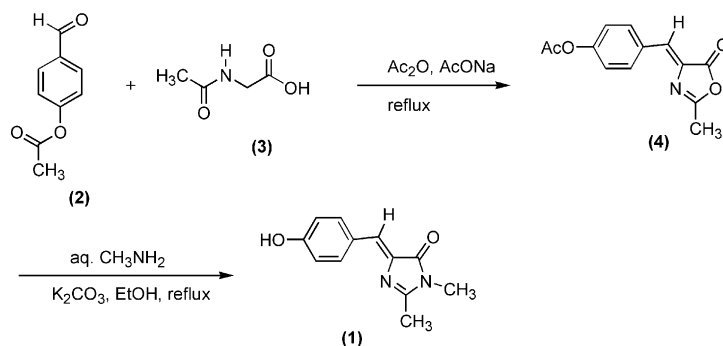
Fig. 1. Preparation of the model chromophore.

sufficiently pure (^{1}H NMR) to be used for the next reaction. Reaction of (4) with a 20-fold excess of 40% aq. methylamine was carried out in the presence of an equimolar amount of anhydrous sodium carbonate in ethanol as a solvent at the reflux (5 h) [19]. The reaction mixture was concentrated under vacuum, acidified at pH 3–4, then extracted with ethyl acetate. The pure product (TLC: SiO_2, ethyl acetate; rf = 0.61) was obtained in 80% yield after recrystallization from ethyl acetate. ^{1}H and ^{13}C NMR analyses confirmed the structure and the chemical purity of (1).

2.2. Sample preparation and SERS spectroscopy

The vibrational features of GFPs were investigated by SERS, exploiting the finding that adsorption of the proteins onto nanometer-sized metallic particles causes an extensive quenching of the fluorescence and gives rise to a dramatic enhancement of the Raman cross-section [20–23]. Solutions of colloidal silver were prepared by standard citrate reduction of $AgNO_3$ (Sigma) by following the procedure of Lee and Meisel [24]. NaCl was added as activation agent to reach the final concentration of 0.25 mM. The colloidal extinction spectrum reveals the same features reported in literature [25,26]. Accordingly, the concentration of silver particles can be estimated to be about 10^{-11} M corresponding to about 7×10^{12} particles per liter. Silver colloidal particles immobilized under ambient conditions were characterized by atomic force microscopy (AFM) in

tapping mode. The colloids consist of single spherical and rod-shaped particles and aggregates of two, three, four up to many particles (the average size is about 70 nm).

The GFP variants EGFP and E^2GFP were a gift of Dr. Mudit Tyagi (International Centre of Genetic Engineering and Biotechnology, Trieste, Italy) and Prof. Mauro Giacca (NEST-INFM and Scuola Normale Superiore, Pisa, Italy) [16].

EGFP and E^2GFP colloidal samples were prepared by adding aliquots of protein solution, at a concentration of 70 μM, to the colloidal solution to reach a final protein concentration of about 5 μM for both samples. The latter were analyzed after a 3-h long incubation. Silver colloids were incubated with the chromophore, previously dissolved in water or in ethanol, at a concentration of 1 mM in order to prepare the chromophore colloidal samples.

Raman and SERS spectra were recorded with a Jobin-Yvon Labram confocal system by exciting with the 632.8 nm radiation line of a He–Ne 20 mW laser. The microscope (equipped with a 100× objective with NA = 0.9) is coupled confocally to a 300 mm focal length spectrograph with a 1800 grooves/mm grating (optimized in the red). A CCD detector Peltier-cooled to 223 K was employed to record the data. The spectral resolution was better than 3 cm^{-1}.

2.3. Computational methods and model systems

Calculations were performed within the density functional theory (DFT) framework, using the

Becke–Lee–Yang–Parr exchange and correlation functional [27]. Valence electron orbitals were expanded in plane waves and core electrons were treated within a pseudopotentials approach [28,29]. Harmonic vibrational frequencies, eigenmodes, and Raman intensities were calculated using density functional perturbation theory [30] and numerical differentiation (using finite displacements of ± 0.01 a.u.) [31]. CPMD3.4.3 [32,33] and the PWSCF package [34] were used for the calculations.

The isolated model chromophore (compound (1) in Fig. 1) was used as basic model. Models for EGFP and E^2GFP active sites were obtained by adding the residues represented in Fig. 2. Starting configurations were taken from representative structures of molecular dynamics trajectories of EGFP and E^2GFP [35]. The molecular dynamics simulations were performed using the Amber6 force field and simulation package [36] and starting from homology modelled structures of EGFP and E^2GFP as described in [35]. The representative structures were chosen by clustering snapshots (taken at each ps) of the 1 ns trajectories using the program NMRCLUST [37]. A 100-step minimization was performed for a preliminary relaxation prior to the DFT based structural optimization and vibrational calculation on the active sites. The cut bonds at the active site boundary were saturated with methyl groups which were kept fixed during the first principle calculations.
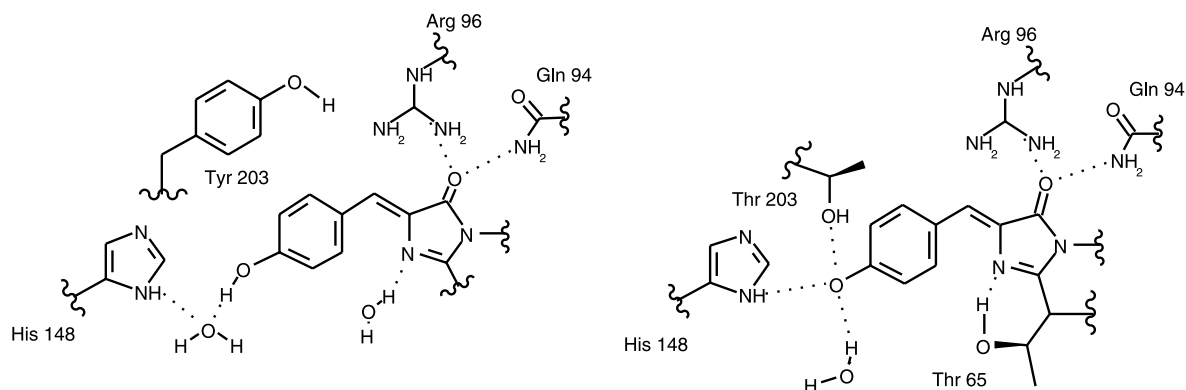
3. Results and discussion

3.1. Chromophore protonation states

Fig. 3 shows the absorption spectrum of the GFP chromophore at a concentration of 50 μM in both aqueous (dotted line) and ethanol (solid line) solution at pH = 7. Both spectra show a band centered at 370 nm. This band is related to the neutral state, while the absence of any feature at larger wavelength indicates that the anionic species is not present as expected in such neutral pH solutions [14,39].
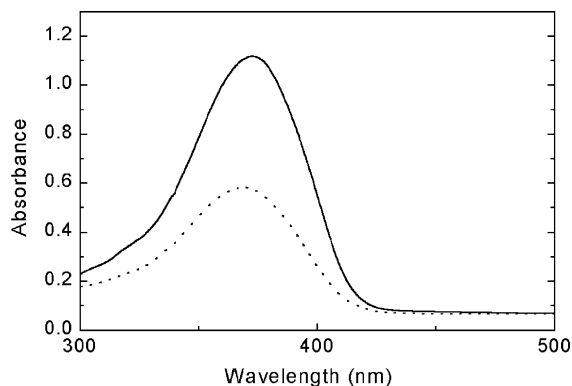
Fig. 3. Absorption spectra of the model chromophore in water (dotted line) or in ethanol (solid line) at a concentration of 50 μM and at pH = 7.

Fig. 2. Schematic representation of the active sites of E^2GFP in A state (left panel) and the EGFP in state B (right panel). The wavy lines represent the sites of covalent linkage with the protein backbone.

The absorption spectra of EGFP and E^2GFP have been presented by some of us elsewhere [17]. The relative A/B populations are very different and the ratio between them is almost reversed in the two mutants, being about 4/1 in E^2GFP and about 1/4 in EGFP. The destabilization of B state in E^2GFP with respect to EGFP stems from mutation T203Y which eliminates the Thr203 hydrogen bond with the chromophore in the B state [38]. This allows us to study separately the vibrational properties of B and A configuration.

3.2. SERS spectra of the chromophore

Fig. 4 shows the SERS spectrum of the chromophore dissolved in water (dashed line) and in ethanol (solid line), at a concentration of 1 mM. The two chromophore SERS spectra are quite similar, in agreement with the fact that the chromophore is present in the neutral form in both cases.

The SERS spectra of the chromophore show a very complex structure. The most intense peaks are found at 606, 1030 and 1162 cm^{-1}, but many other less intense peaks are detected throughout the spectrum. In the frequency range where data are available, most of the structure finds a correspondence to reported Raman or resonant Raman
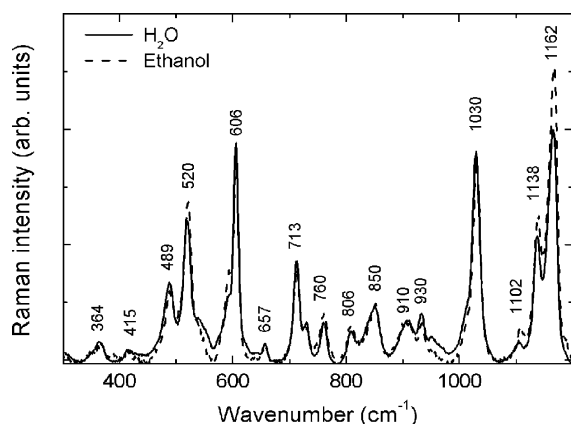
data for the chromophore in solution [14]. SERS technique, however, yields a much enhanced signal in the 400–700 nm spectral region, where a detailed analysis with the conventional Raman techniques is not possible, due to the low signal-to-noise ratio.

3.3. SERS spectra of the proteins

Fig. 5 shows representative SERS spectra of EGFP (dashed line) and E^2GFP (solid line), whereas the conventional Raman spectra are shown in the inset, for comparison. The latter are very similar for EGFP and E^2GFP and show a large background over which broad bands can be detected. The only evident detectable band is located in the 500–700 cm^{-1} region. The presence of a significant background stemming from the intrinsic fluorescence of the molecules drastically shadows the Raman signal. We stress that the colloidal Ag solution does not reveal any Raman signal (results not shown). In fact the marked vibrational features observable in the SERS spectrum of Fig. 5 are due to the GFP molecules: the reduction of the fluorescence background yields the observed well-resolved signal. Similar effects, together with a strong enhancement of the Raman
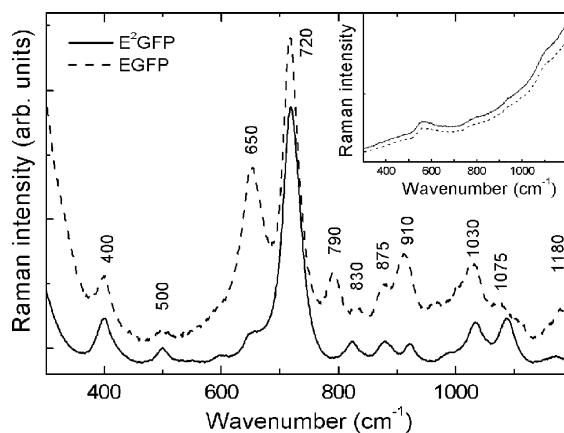

Fig. 4. SERS spectra of the model chromophore in silver colloidal solution at a concentration of 50 μM, previously dissolved in water (solid line) and in ethanol (dashed line). Both the spectra have been obtained with an integration time of 10 s and exciting at 632.8 nm.

Fig. 5. SERS spectra of EGFP (dashed line) and E^2GFP (solid line) silver colloidal solution at a concentration of 5 μM. Both spectra have been obtained with an integration time of 10 s and exciting at 632.8 nm; a vertical shift has been applied to the E^2GFP spectrum. In the inset: Raman spectra of EGFP and E^2GFP in phosphate buffer solution at a concentration of 5 μM, obtained exciting at 632.8 nm.

cross-section, were reported in the case of rhodamine and other dyes [22]. This enhanced sensitivity is pivotal to allow our analysis of the Raman spectra and to perform a meaningful comparison between the data relative to the two different mutants.

Many of the recorded vibrational features are common to EGFP and E^2GFP SERS spectra. In particular, both spectra show a dominant band located at 720 cm^{-1}. Significantly, however, differences between EGFP and E^2GFP can be detected at some specific frequencies and in the relative intensities of the peaks. In particular, the 650 cm^{-1} band has a much weaker intensity in E^2GFP and the 790 cm^{-1} band is altogether absent [40]. In the higher frequency region where such a comparison can be made, our data are in qualitative agreement with those reported in the literature [13,14].

A comparison between Figs. 4 and 5 reveals a general broadening and a strong suppression of the bands in the range 1030–1162 cm^{-1} and in the range 489–600 cm^{-1} in the protein data with respect to the chromophore. Even if weakened and broadened, however, most of the bands visible in the proteins find a correspondence in those of the chromophore. This is to be expected since the latter is the dominantly absorbing structure of the protein at the exciting wavelength chosen.

In the following section we shall analyze the origin of the differences between protein and chromophore spectra on the structural basis.

3.4. Calculations, mode assignment and discussion

Table 1 reports the experimental and calculated vibrational Raman-active modes. Protein models shown in the left and right panels of Fig. 6 were chosen for E^2GFP and EGFP, respectively: they represent the configurations of the dominantly populated states in the two mutants. The neutral chromophore was chosen as the model for the chromophore in solution. In order to present our data we grouped in bands (v_i) modes with similar displacement pattern and frequency. The last row of Table 1 shows the calculated Raman intensities of each band as histograms. A quantitative agreement is found with the measured band intensities of

the chromophore in solution (Fig. 4) in the range above 1000 cm^{-1}. Below 1000 cm^{-1}, the calculated intensities are much weaker, since the SERS enhancement is not included. The relative intensities within this range, however, are well reproduced.

Previous attempts to assign GFP vibrational bands focused on the high-frequency region of the spectrum (1400–1700 cm^{-1}). Here a few Raman-active bands are clearly distinguishable and were assigned to C=O, C=C, C=N and phenolic C—C bond stretching on the basis of DFT-based calculations of frequency and Raman intensity of the isolated model chromophore [41,42]. We adopted the same assignment strategy, but we performed our calculations on the model proteins as well. We took advantage of these additional calculations and the comparison of these results with respect to those of the isolated chromophore as a further criterion to assign modes. The agreement between theoretical and experimental frequencies is on average within 3–5%. We observe that interactions of the active site can split a given chromophore mode in two or more modes with similar frequencies and patterns of vibration, or can couple and merge two chromophore modes in a single broader band. From the experimental point of view, these effects contribute to the already mentioned broadening of the protein spectrum with respect to the chromophore.

The bands can be classified in three groups: (a) those which are present both in the proteins and in the chromophore in solution (albeit broadened and shifted in frequency), (b) bands which are depressed and/or largely shifted in frequency in the proteins with respect to the chromophore in solution, (c) bands which are characteristic of the proteins. The three letters (a)–(c) were used to label the bands in Table 1. A more detailed analysis of some "fingerprint" bands follows, based on our assignment. Starting from group (a), the main band in the protein spectrum (v_8) is observed at 720 cm^{-1}, while in the same range of frequency we find three distinct modes in the chromophore. These can be assigned to largely planar deformations of both rings (see Fig. 6) of the chromophore which are highly coupled and mixed in the protein models. This intense band can be considered characteristic of the GFP family, since it involves a collective vibration of the double ring structure

Table 1
Experimental and theoretical Raman active bands

	$\nu_1^{(a)}$	$\nu_2^{(b)}$	$\nu_3^{(b)}$	$\nu_4^{(b)}$	$\nu_5^{(b)}$	$\nu_6^{(b)}$	$\nu_7^{(c)}$	$\nu_8^{(a)}$	$\nu_9^{(c)}$	$\nu_{10}^{(b)}$	$\nu_{11}^{(a)}$	$\nu_{12}^{(c)}$	$\nu_{13}^{(a)}$	$\nu_{14}^{(b)}$	$\nu_{15}^{(c)}$	$\nu_{16}^{(b)}$	$\nu_{17}^{(b)}$
Experiment																	
CRO	364	415	489	520	(585) 606	657		713 720 760		806	850		910 930	(1010) 1030		1102 1138	1162
E²GFP	400		500	500	(595)	(650)		720		830	875		910	1030	1090		1180
EGFP	400		500	500		(650)	650	720	790	830		(875)	910	1030	1075 (1110)		1180
Theory																	
CRO	386	412	447 501	509	558 590	634		694 729 732		785	839		907	1012 993 976		1083 1104	1156 1163 1167
E²GFP(A)	344 467	434 468	524 536 542	503		637 640		657 719		808	820 821 840	883 906	918	990 1001	1085	1133 1146	1206 1222
EGFP(B)	389	489 500	421 485 530	479 521		622	642	671 691 741	780	812	828		924	1036 1043	1126	1114 1136	1162

Raman intensity (Theory)

The bands are numbered and classified in groups (a), (b) and (c) (see text). The theoretical values for CRO, E²GFP(A) and EGFP(B) correspond to the isolated model chromophore and to models in Fig. 2, respectively (see text). Frequencies are in cm^{-1}. Values in parenthesis are shoulders or small peaks. The histograms in the last row represent the calculated Raman intensities of the isolated neutral chromophore, summed over the modes in each band (arbitrary units).
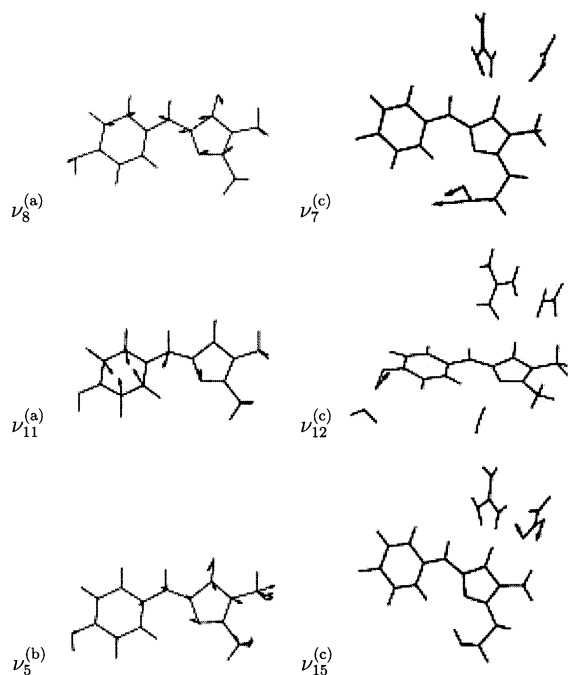
Fig. 6. Representation of the pattern of displacement of some of the chromophore and protein modes.

which is present only in these proteins. Also characteristic is the band ν_{11} (at 850 cm^{-1} in the chromophore in solution, shifted at lower frequencies in the proteins). This can be associated to a planar "breathing" mode of the chromophore transverse with respect to its longitudinal axis (see Fig. 6).

Moving to group (b), the most evident suppression in passing from the chromophore to the protein is the band ν_5 appearing at 606 cm^{-1} in the chromophore, but almost completely absent in the protein. The corresponding calculated mode is a planar deformation mainly localized on the imidazolidinone ring involving also the motion of the methyl groups. This is indeed absent in the model proteins due to the absence of methyl groups and to the constraints imposed by the linkage with the protein backbone (see Fig. 6). Bands ν_2, ν_3, and ν_4 involve motion of the phenolic oxygen and related hydrogen, thus these appear either suppressed or strongly shifted in the protein due to the presence of hydrogen bonds. Bands ν_{14}, ν_{16} and ν_{17} involve C—C and C—N stretching and planar deformation of the imidazolinone ring, thus are either depressed

or shifted in the protein owing to the backbone constraints.

Group (c) includes the vibrational bands peculiar to the proteins (absent in the chromophore in solution) and is of particular interest to shed light on the protein structure. Band ν_{15} can be associated with a mode localized on the NH$_2$ group of Gln94 which is hydrogen bonded to C=O group of the chromophore (see Fig. 6). ν_7 (650 cm^{-1}), ν_9 (790 cm^{-1}) and ν_{12} (875 cm^{-1}) bands deserve special attention. ν_9 is mainly present in EGFP and ν_7 is particularly enhanced in EGFP with respect to E^{2}GFP [40]. These bands should be associated to state B which is dominantly populated in EGFP, but little populated in E^{2}GFP. Indeed the calculated modes associated to ν_9 and ν_7 are typical of state B: they involve angular motions of the protons hydrogen-bonding the phenolate oxygen (ν_9) and of the C—OH group of Thr65, hydrogen bonded to the imidazolidinone ring nitrogen (ν_7, see Figs. 2 and 6). According to our calculations, the weak peak present at 657 cm^{-1} in the chromophore in solution is due to another band with low Raman intensity (ν_6) corresponding to planar angular deformation of the phenolic ring. Finally band ν_{12} is an angular mode of the chromophore phenolic hydrogen also hydrogen-bonded to a water molecule (see Fig. 6), thus is typical of state A. The presence of a shoulder also in EGFP can be explained with the vibrations of Gln94 and Arg96 hydrogens (data not shown), which are predicted to be at almost the same frequency, both in EGFP and E^{2}GFP models.

4. Conclusions

In this paper we have reported an extensive study of the vibrational properties of the EGFP and E^{2}GFP in the range 300–1200 cm^{-1} exploiting the Raman intensity enhancement produced in the SERS technique. The comparison with the synthetic chromophore spectrum in solution revealed some modes peculiar of the protein states and the depression or change in frequency of several chromophore bands within the protein environment. These spectral differences were clarified on the basis of the mode assignment to specific pat-

terns of vibrations, based on first principle calculations. A characteristic GFP band at 720 cm^{-1} was associated to a collective planar deformation of the chromophore. Furthermore, we identified some fingerprint modes differentiating A and B states of the proteins, namely bands at 650 and 760 cm^{-1} and at 875 cm^{-1}. These bands reflect the conformation of the local chromophore environment. In particular, the band at 650 cm^{-1} corresponds to the vibration of the proton in proximity of the heterocyclic nitrogen in B state, which has been proposed to be involved in the blinking process. Monitoring the evolution of this vibrational mode during blinking events may shed light on the nature of the dark state associated to the blinking process.

In general, our study indicates that it is possible to characterize the chromophore states in the protein by means of the analysis of the low frequency spectrum. An advantage of exploring this range of frequency is that it includes delocalized collective angular modes which are typical of the double ring structure of the chromophore. These are typified by the 720 cm^{-1} band, which is particularly strong and could be used to monitor photo-induced structural rearrangements of the chromophore. This opens new routes to the structural characterization of the GFP sub-states or dark states. Moreover the dominant band at 720 cm^{-1} could allow the use of SERS to complement GFP fluorescence in advanced imaging applications.

Acknowledgements

References

[1] R.J. Tsien, Annu. Rev. Biochem. 67 (1998) 509.

[2] M. Zimmer, Chem. Rev. 102 (2002) 759.

[3] O. Shimonmura, F.H. Johnson, Y. Saiga, J. Cell. Comp. Physiol. 59 (1962) 223.

[4] A. Zumbush, G. Jung, Single Mol. 1 (2000) 261.

[5] M. Ormö, A.B. Kubitt, K. Kallio, L.A. Gross, R.Y. Tsien, S.J. Remington, Science 273 (1996) 1392.

[6] R. Heim, D.C. Prasher, R.Y. Tsien, Proc. Natl. Acad. Sci. USA 91 (1994) 12501.

[7] K. Brejc, T.K. Sixma, P.A. Kitts, R.K. Steven, R.Y. Tsien, M. Ormö, S.J. Remington, Proc. Natl. Acad. Sci. USA 94 (1997) 2306.

[8] R.M. Dickson, A.B. Cubitt, R.Y. Tsien, W.E. Moerner, Nature 388 (1997) 355.

[9] A.A. Voityuk, M.E. Michel-Beyerle, N. Rösh, Chem. Phys. 231 (1998) 13.

[10] W. Weber, V. Helms, J.A. McCammon, P. Langhoff, Proc. Natl. Acad. Sci. USA 96 (1999) 6177.

[11] R. Nifosì, A. Ferrari, C. Arcangeli, V. Tozzini, V. Pellegrini, F. Beltram, submitted.

[12] J.J. van Thor, A.J. Pierik, I. Nugteren-Roodzant, A. Xie, K.J. Hellingwerf, Biochemistry 37 (1998) 16915.

[13] A.F. Bell, X. He, R.M. Wachter, P.J. Tonge, Biochemistry 39 (2000) 4423.

[14] P. Schellenberg, E. Johnson, A.P. Esposito, P.J. Reid, W.W. Parson, J. Phys. Chem. B 105 (2001) 5316.

[15] R.A.G. Cinelli, V. Tozzini, V. Pellegrini, F. Beltram, G. Cerullo, M. Zavelani-Rossi, S. De Silvestri, M. Tyagi, M. Giacca, Phys. Rev. Lett. 86 (2001) 3439.

[16] R.A.G. Cinelli, A. Ferrari, V. Pellegrini, M. Tyagi, M. Giacca, F. Beltram, Photochem. Photobiol. 71 (2000) 771.

[17] R.A.G. Cinelli, V. Pellegrini, A. Ferrari, P. Faraci, R. Nifosì, M. Tyagi, M. Giacca, F. Beltram, Appl. Phys. Lett. 79 (2001) 3353.

[18] J.S. Buck, W.S. Ide, Org. Synth. Coll. 2 (1943) 55.

[19] S. Kojima, H. Ohkawa, T. Hirano, S. Maki, H. Niwa, M. Ohashi, S. Inouye, F.I. Tsuji, Tetrahedron Lett. 39 (1998) 5239.

[20] H. Xu, E.J. Bjerneld, M. Kaell, L. Boerjesson, Phys. Rev. Lett. 83 (1999) 4357.

[21] S. Nie, S.R. Emory, Science 275 (1997) 1102.

[22] K. Kneipp, H. Kneipp, I. Itzkan, R.R. Dasari, M.S. Feld, Chem. Rev. 99 (1999) 2957.

[23] A.R. Bizzarri, S. Cannistraro, Appl. Spectrosc., in press.

[24] P. Lee, C. Meisel, J. Phys. Chem. 86 (1982) 3391.

[25] P. Hildebrandt, M. Stockburger, J. Phys. Chem. 88 (1984) 5935.

[26] A.M. Michaels, M. Nirmal, L.E. Brus, J. Am. Chem. Soc. 121 (1999) 9939.

[27] D.A. Becke, Phys. Rev. A 38 (1988) 3098;
C. Lee, W. Yang, R.G. Parr, Phys. Rev. B 37 (1988) 785.

[28] We used Troullier–Martins pseudopotentials [N. Troullier, J.L. Martins Phys. Rev. B 43 (1991) 1993–2006] with core radius 1.23 a.u. for C and N and 1.25 for O. The pseudopotential for H was obtained as in [L. Pavesi, P. Giannozzi, F.K. Reinhart, Phys. Rev. B 42 (1990) 1864–1867]. This set of pseudopotentials lead to a convergence of the geometry within $\leqslant 0.3\%$ of the full convergence values at 60 Ry of energy cutoff for the plane waves. A test

calculation on formaldehyde showed that the experimental vibrational frequencies are reproduced with an average accuracy of 3%.

[29] Orthorhombic simulation boxes with cell sides varying from 30 to 40 a.u. were chosen depending on the model system in order to leave at least 5 Å of empty space between periodic images.

[30] S. Baroni, S. de Gironcoli, A. Dal Corso, P. Giannozzi, Rev. Mod. Phys. 73 (2001) 515.

[31] P. Giannozzi, S. Baroni, J. Chem. Phys. 100 (1994) 8537.

[32] R. Car, M. Parrinello, Phys. Rev. Lett. 55 (1985) 2471.

[33] CPMD3.4: J. Hutter, A. Alavi, T. Deutsch, P. Ballone, M. Bernasconi, P. Focher, E. Fois, S. Goedecker, D. Marx, M. Parrinello, M. Tuckerman, MPI für Festkörperforschung, Stuttgart and IBM Zurich Research Laboratory.

[34] S. Baroni, A. Dal Corso, S. de Gironcoli, P. Giannozzi, Available from <http://www.pwscf.org>.

[35] R. Nifosì, V. Tozzini, Proteins, in press.

[36] D. Case, D. Pearlman, J. Caldwell, T. Cheatham III., W. Ross, C. Simmerling, T. Darden, K. Merz, R. Stanton, A. Cheng, J. Vincent, M. Crowley, V. Tsui, R. Radmer, Y. Duan, J. Pitera, I. Massova, G. Seibel, U. Singh, P. Weiner, P.A. Kollman, Amber 6.0. (1999).

[37] L.A. Kelley, M.J. Sutcliffe, Protein Eng. 9 (1996) 1063.

[38] M.R. Wachter, M.A. Elsliger, K. Kallio, G.T. Hanson, S.J. Remington, Structure 6 (1998) 1267.

[39] A.A. Voityuk, A.D. Kummer, M.-E. Michel-Beyerle, N. Rösch, Chem. Phys. 269 (2001) 83.

[40] Some specific bands, such as 650 and 790 cm^{-1} show a certain degree of variability in their relative intensity, depending on sample preparation and on their story prior to illumination. We attribute this to fluctuations in relative A/B population.

[41] A.P. Esposito, P. Schellenberg, W.W. Parson, P.J. Reid, J. Mol. Struct. 569 (2001) 25.

[42] V. Tozzini, R. Nifosì, J. Phys. Chem. B 105 (2001) 5797.